International Journal of Nanomedicine Dovepress

Open Access Full Text Article ORIGINAL RESEARCH

Penetration Enhancer-Free Mixed Micelles for Improving Eprinomectin Transdermal c Efficiency in Animal Parasitic Infections Therapy

Yujuan Mao[1,*], Tianjiao Hao[2,*], Hongxiu Zhang[2,*], Xiaofei Gu[2], Jing Wang[1], Feifei Shi[1], Xiaolan Chen[1], Liuna Guo[1], Jie Gao[1], Yan Shen[2], JinLin Zhang[3], Shenglan Yu[4]

[1]Jiangsu Agri-Animal Husbandry Vocational College, Taizhou, Jiangsu, 225300, People's Republic of China; [2]Department of Pharmaceutics, China Pharmaceutical University, Nanjing, 210009, People's Republic of China; [3]Jiangsu Institute for Food and Drug Control, Nanjing, Jiangsu Province, 210019, People's Republic of China; [4]College of Animal Medicine, Jiangsu Agri-Animal Husbandry Vocational College, Taizhou, People's Republic of China

*These authors contributed equally to this work

Correspondence: Shenglan Yu; JinLin Zhang, Email slyu70@126.com; zjluser@126.com

Introduction: Eprinomectin offers promise against parasitic infections. This study develops Eprinomectin (EPR) mixed micelles for transdermal delivery, aiming to enhance efficacy and convenience against endoparasites and ectoparasites. Physicochemical characterization and pharmacokinetic studies were conducted to assess its potential as an effective treatment for parasitic infections.

Methods: Blank and EPR mixed micelles were prepared using PEG-40 Hydrogenated castor oil (RH-40) and Nonyl phenol polyoxyethylene ether 40 (NP-40). Critical micelle concentrations (CMC) determined using the pyrene fluorescence probe method. Particle size, EE, DL, in vitro release, permeation, and skin irritation were evaluated. In vivo pharmacokinetic studies were conducted in male Sprague-Dawley rats.

Results: Results show that EPR mixed micelles present suitable stability, physicochemical properties, and safety. Moreover, the rapid release and high bioavailability of EPR mixed micelles have also been verified in the study. Pharmacokinetic experiments in vivo showed that an improvement in the transdermal absorption and bioavailability of EPR after encapsulation in mixed micelles formulations.

Conclusion: The results proved that the novel mixed micelles are safe and effective and are expected to become a promising veterinary nano-delivery system.

Keywords: eprinomectin, mixed micelles, transdermal delivery, pharmacokinetics

Introduction

Parasites pose a greater health threat than bacteria, often leading to chronic diseases in both humans and livestock.[1] Once parasitized, livestock and poultry suffer from nutrient consumption, fostering parasite growth and escalating feed costs.[2] Australia, a major meat-exporting nation, annually incurs approximately AUD 1 billion in losses due to parasitic infections.[3] Challenges in timely diagnosis of parasitic infections result in significant economic losses in livestock farming.[4,5] Parasites, distinct from bacteria, present zoonotic transmission risks, impacting human health.[6] With complex life cycles involving intermediate hosts and varying drug sensitivities across growth stages, parasitic infections prove challenging to treat effectively.

Eprinomectin (EPR) represents a hydrophobic 16-membered macrocyclic lactone antibiotic developed by Merck.[7] EPR, as a commonly used broad-spectrum antiparasitic drug in veterinary medicine, exhibits stronger efficacy, higher safety, and lower resistance development compared to avermectin-class drugs like ivermectin and abamectin.[8,9] It demonstrates potent parasiticidal effects against various parasites and finds extensive use in the prevention and treatment of parasitic diseases in animals such as cattle, sheep, camels, pigs, rabbits, and dogs.[10] Notably, EPR exhibits high safety in mammals, marking it as

Received: 16 July 2024
Accepted: 25 October 2024
Published: 1 November 2024

the first low-residue green veterinary drug applicable to dairy and meat-producing livestock without withdrawal periods, thus exhibiting considerable potential for research and development.[11,12] Traditionally, antiparasitic drugs have predominantly existed in conventional formulations such as powders, tablets, premixes, and injections. Oral administration constitutes a critical method for controlling gastrointestinal parasitic infections in animals.[13,14] However, these conventional formulations often necessitate frequent administration, result in a short duration of efficacy, and induce the significant "peak-valley" phenomenon in blood drug concentrations, thereby causing substantial toxic side effects. With advancements in transdermal delivery, the development of efficient, low-toxicity, and long-acting formulations for antiparasitic drugs has become a research focus. Transdermal formulations, including transdermal patches, have garnered significant attention. Compared to other administration methods, transdermal formulations offer three advantages,[15–17] (1) avoidance of the hepatic first-pass effect and gastrointestinal inactivation associated with oral administration; (2) reduction of individual variations to maintain a constant blood drug concentration, prolonging drug action time and enhancing efficacy; (3) convenient usage with the ability to promptly halt administration in case of issues.

EPR demonstrates good transdermal absorption, enabling widespread distribution throughout the body to exert its therapeutic effects, rendering it an ideal candidate for transdermal formulations.[18–20] Presently, commercial formulations of EPR abroad include Merial's 0.5% pour-on formulation Eprinex® and 5% injectable formulation LongRange®.[21,22] Although injectable formulations exhibit higher bioavailability, their administration is inconvenient and causes significant disturbance to animals. Extensive investigations have explored drug delivery via micelles carriers across various routes such as parenteral, oral, ocular, pulmonary, and nasal administration.[23] Recent research has also focused on employing micelles carriers for targeted cutaneous delivery of active compounds, exhibiting promise in treating dermatological conditions like psoriasis,[24,25] fungal infections,[26] and acne.[27] Studies have elucidated the deposition of micelles carriers, particularly those comprising PEG-dihexPLA, in the skin, with the follicular pathway identified as the primary transport route.[23,28] However, investigations into the skin delivery and follicular targeting of mixed micelles based on FDA-approved Pluronic® F127 polymer remain limited. Further research endeavors in this domain hold the potential for enhancing the efficacy and specificity of drug delivery systems, thus addressing constraints associated with conventional methodologies. When different types of surfactants are mixed, they complement each other to form a more stable micelles structure. This structure exhibits better resistance to ionic strength and temperature, reducing micelles aggregation and drug precipitation, thus enhancing the formulation's stability. Furthermore, mixed surfactants can enhance the water solubility and dissolution rate of drugs, making poorly soluble drugs more easily encapsulated and released. This enhanced solubility contributes to improved stability and dissolution of the drug. In addition, the barrier effect of the stratum corneum is the most powerful among all layers of the skin. Excipients such as Azone can disrupt the arrangement of lipids in the corneous layer, leading to cracking of lipid coating on cells and facilitating drug penetration. However, these permeability enhancers may also have stimulating effects while improving skin permeability. Amphiphilic micelle, a novel type of nanomedicine transdermal delivery system, offer advantages in terms of stability and skin penetration. In this study, the EPR mixed micelles prepared have a particle size smaller than 20 nm, allowing them to pass through intercellular spaces of the stratum corneum passively while maintaining their structure intact and penetrating deep into the dermis. Additionally, nonionic surfactants RH-40 and NP-40 in mixed micelles enhance fluidity of the lipid layer in the corneous layer, increase skin surface permeability, and further promote drug penetration for efficient transdermal drug delivery.[29]

This study focused on the preparation and characterization of penetration enhancer-free EPR mixed micelles for transdermal delivery. As shown in Scheme 1, blank mixed micelles and EPR-loaded mixed micelles were prepared using a combination of surfactants and ethanol, followed by hydration. The CMC of the surfactants was determined using the steady-state fluorescence method. Particle size and distribution of the mixed micelles were evaluated using dynamic light scattering (DLS) and transmission electron microscopy (TEM). Encapsulation efficiency (EE) and drug loading (DL) were quantified, and EPR concentration was determined using high performance liquid chromatography (HPLC). In vitro drug release, permeation, and skin irritation tests were conducted to assess the performance of EPR mixed micelles. Pharmacokinetic studies were performed in rats to compare the transdermal delivery of EPR mixed micelles with 0.5% pour-on formulation Eprinex. Overall, the study aimed to develop an effective transdermal delivery system for EPR, addressing challenges in parasitic infection treatment.

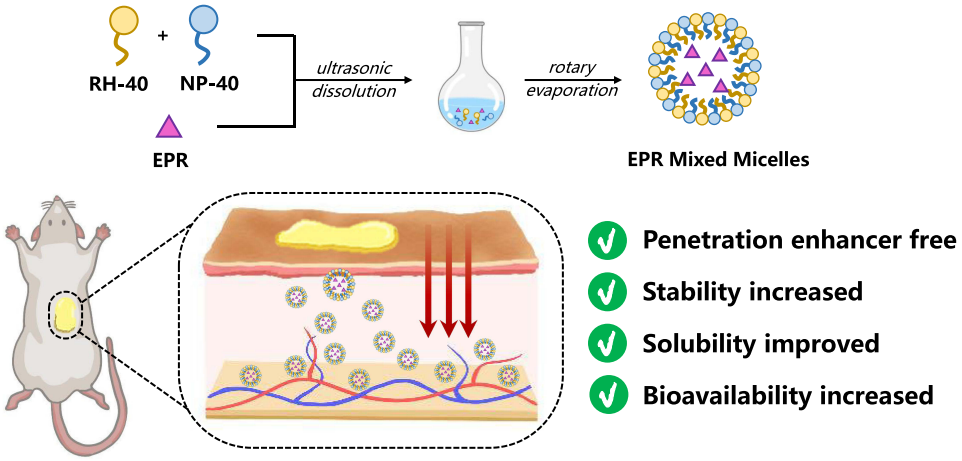

Scheme 1 Preparation and evaluation of mixed micelles.

Materials and Methods

Material and Animals

EPR (B1a+B1b≥95%, B1a≥90%) was procured from North China Pharmaceutical Group Aino Co., Ltd. (Shijiazhuang, China). Polyoxyl 40 Hydrogenated Castor Oil (RH-40) was obtained from BASF, Germany, while nonylphenol polyoxyethylene ether 40 (NP-40) was acquired from Pan Asia Chemical Corporation. Ethanol was sourced from Nanjing Chemical Reagent Co., Ltd. (Nanjing, China). Acetonitrile (chromatographically pure) was purchased from TEDIA Corporation, USA. Animals were obtained from Nanjing Qinglongshan Experimental Animal Center (Nanjing, China). All animal experiments were conducted following the guidelines for the care and use of laboratory animals set by the National Institutes of Health, USA, and approved by the Animal Ethics Committee of China Pharmaceutical University (2023–05-31).

Methods

Determination of Critical Micelle Concentration (CMC)

This study employed the pyrene fluorescence probe method to determine the critical micelle concentration. The fluorescence emission spectrum of the pyrene solution exhibited five absorption peaks near 373 nm, 379 nm, 383 nm, 390 nm, and 480 nm. Changes in the ratio of the intensity of the first emission peak I_1(373 nm) to the third emission peak I_3 (383 nm) with variations in the polarity of the pyrene environment were indicative of changes in the impact of the micelles structure on the fluorescence of the pyrene probe. Therefore, the ratio I_1/I_3 was determined, and the CMC values of various micelle systems were compared by calculating the ratio of the two. Using the fluorescence spectrum intensity of pyrene as the y-axis (I_1/I_3) and the logarithmic value log(c) of the micelle solution as the x-axis, a curve was fitted using Origin 8.5 software. The change trend of the curve conforms to the Boltzmann (Equation 1),

$$\frac{I_1}{I_3}=\frac{A_1-A_2}{1+e^{(x-x_0)/dx}}+A \tag{1}$$

where A_1 and A_2 are the maximum and minimum values of I_1/I_3 respectively, X is the concentration of surfactant solution, X_0 is the midpoint of curve mutation, dx is the parameter of curve mutation degree. The concentration corresponding to X_0 is the critical micelle concentration of the sample.

Preparation of Blank Mixed Micelles and EPR Mixed Micelles

To prepare both blank and EPR-loaded mixed micelles, 2.00 g of RH-40 and 0.10g of NP-40 were accurately weighed and ultrasonically dissolved in 3 mL of ethanol in a flask. The dissolution process occurred at 40°C with rotary evaporation (RE-52AA, Shanghai Yarong Biochemistry Instrument Factory, Shanghai, China) for 30 minutes, removing

the ethanol until a thin film formed on the inner wall of the flask. Subsequently, water was added to reach a total weight of 50g, and thorough mixing was performed. The mixture then underwent hydration through magnetic stirring (85–2, Shanghai Sile Instrument Co., Ltd, Shanghai, China) at a speed of 1500 r/min for 4 hours, resulting in the formation of both blank and EPR-loaded mixed micelles. For the preparation of EPR-loaded mixed micelles, 0.25 g of EPR was additionally ultrasonically dissolved in ethanol before being combined with the RH-40 and NP-40 solutions.

Particle Size and Distribution Determination

The particle size and distribution of the prepared blank mixed micelles and EPR mixed micelles were determined by placing them separately in size and zeta potential dishes. Measurements were conducted in triplicate using a DLS particle size analyzer from Brookhaven Instruments at 25°C and a scattering angle of 90°. For each sample, the average particle size (nm), polydispersity index (PDI), and mean zeta potential (mV) were recorded.

Tem

The microstructures of the mixed micelles were characterized using transmission electron microscopy (TEM, HT7700, Hitachi Japan). Briefly, measured quantities of both blank mixed micelles and EPR mixed micelles were dropped onto copper grids coated with a carbon film. After complete wetting for 5 minutes, excess liquid was removed with filter paper. Subsequently, negative staining was performed using a 1% (w/v) sodium phosphotungstate solution. After a 5-minute incubation, excess staining solution was removed with filter paper, and the grids were air-dried under infrared light for approximately 3 minutes. Subsequently, the samples were analyzed and imaged using a transmission electron microscope.

Fourier Transform Infrared Spectroscopy (FT-IR)

FT-IR (Brook, TENSOR27) is used to study the structural characteristics of drugs and surfactants to verify whether the drug is successfully encapsulated in micelles. The blank mixed micelles and EPR mixed micelles were freeze-dried. The freeze-dried powders of blank mixed micelles, EPR mixed micelles, and EPR raw materials were mixed with potassium bromide, ground, and pressed into pellets using a mold. The FT-IR scanning range was between 400 cm^{-1} and 4000 cm^{-1}, and the infrared spectra of EPR raw materials, blank mixed micelles, and EPR mixed micelles were scanned separately.

Encapsulation Efficiency (EE) and Drug Loading (DL) Determination

The encapsulation efficiency of EPR mixed micelles was quantified. Following ultrahigh-speed centrifugation, the supernatant and precipitate of each formulation were analyzed using the phenol sulfuric acid method to determine the unencapsulated drug concentration. Encapsulation efficiency (EE) and drug loading efficiency (DL) of both formulations was subsequently expressed as a percentage, utilizing the following formula(2) and (3),

$$Encapsulation\ Effiency = \frac{Total\ concentration - non\ encapsulated\ drug}{Total\ concentration} \times 100\% \quad (2)$$

$$DL\ Efficiency = \frac{Encapsulated\ drug}{Total\ concentration} \times 100\% \quad (3)$$

EPR concentration was quantified by HPLC using an LC-20ATShimadzu system with autosampler (Shimadzu Corporation, Kyoto, Japan) and a UV detector (Shimadzu, SPD-20A UV/VisDetector, Kyoto, Japan) at 245nm. A Welch Ultimate AQ-C18 colμmn, 5μm (250mm×4.6mm) was used for separation at the column oven temperature of 30 °C. The mobile phase used was comprised of 75% acetonitrile and 25% water at the flow rate of 1 mL/min (isocratic elution). Initially, a series of known concentrations of standard solutions ranging from 0.01 to 25μg/mL were run to draw a calibration curve to quantify the concentration of EPR in test samples.

In vitro Drug Release

In our study, ethanol was found to be suitable for the properties of EPR. Therefore, the solubility of EPR in different media was initially determined. Various release media were prepared and placed in volumetric flasks, into which excess EPR raw material was added and uniformly dispersed through ultrasonication. The mixture was subjected to a 32°C water bath with magnetic stirring. Timed samples were collected, diluted, filtered, and analyzed by HPLC to calculate the drug's solubility in different receptor buffers. The screening of various synthetic artificial membranes was conducted. The receptor buffer was degassed by ultrasonication for 15 minutes, and the degassed receptor buffer was placed in a water bath at 32°C for temperature stabilization. JinTeng MCE 0.2 μm, JinTeng PVDF 0.2 μm, and Cobetter-GF-0.45 μm artificial membranes were incubated in the receptor buffer for 30 minutes, then fixed onto the Franz diffusion cell (RYJ-12B, Shanghai Huanghai Pharmaceutical Inspection Instrument Co., Ltd., Shanghai, China). The effective membrane exposure area of the Franz diffusion cell system was 2.20 cm^2, with a receptor buffer volume of 8 mL, a water bath temperature of 32±0.3°C, and a stirring speed of 600 rpm/min. Continuing, the receptor buffer was injected into the diffusion cell using a syringe, and any bubbles in the diffusion cell were purged. Subsequently, 1 mL of Eprinex and EPR mixed micelles were placed in the sample chamber. At 0.5h, 1h, 2h, 4h, and 6h, 1 mL samples were withdrawn with a syringe, and an equal volume of the receiving medium was replenished. The withdrawn receiving medium was filtered through a 0.22μm membrane, and subjected to injection for detection, and the concentration of EPR (Cn) in the sample chamber was calculated at each time point.

The Higuchi model was employed under the assumption of perfect sink conditions and pseudo-infinite dose. The release amount Qn(4), defined as the amount released per unit area at time (n) in μg/cm^2, was determined using the equation. Here, Cn represents the drug concentration in the receiving medium at different sampling times, Vs is the sample volume, Vc is the diffusion cell volume, and Ac is the membrane exposure area. The artificial membranes were selected based on the R^2 value of the fitted curve.

$$Q_n = C_n \frac{\mathrm{Vc}}{\mathrm{Ac}} + \frac{\mathrm{Vs}}{\mathrm{Ac}} \sum_{i=1}^{n} C_{i-1} \tag{4}$$

The artificial membranes selected from the above experiments were placed in the receiving solution and incubated for 30 minutes, then fixed onto the Franz diffusion cell. Using a syringe, the receiving medium was injected into the diffusion cell, and any bubbles in the diffusion cell were purged. One milliliter each of Eprinex and EPR mixed micelles was placed in the sample chamber, in triplicate. At 0.5h, 1h, 2h, 4h, 6h, and 8h, 1 mL samples were withdrawn with a syringe, and an equal volume of receiving medium was replenished. The withdrawn receiving medium was filtered through a 0.22μm membrane, and subjected to injection for detection, and the concentration of EPR (Cn) in the sample chamber was calculated at each time point. The Higuchi model and formula were employed to calculate Qn, with the release rate as the regression line slope of the square root of the time curve.

In vitro Permeation Study

An in vitro permeation study was conducted to evaluate the permeability of EPR from different formulations. For this, the Franz diffusion cell system with a 2.20cm^2 effective diffusion area was used. Skin without any defects was mounted between donor and receptor compartments in the diffusion cell, with the epidermis side facing the donor compartment (18 weeks old Male ICR mice, Shanghai Bikeyi Biotechnology Co., Ltd., certificate number: No.20230009000067). The receptor compartment was filled with an 8mL receptor buffer (normal saline containing 30% Ethanol). After that, Eprinex and EPR Mixed micelles containing the same quantity of EPR were put separately in the donor compartment. Then the temperature in the diffusion chamber was maintained at 32±0.3°C in a thermostatic water bath and a stirring speed of 600 rpm/min. Samples from receptor chambers were collected at predetermined time intervals (1, 2, 4, 6, 8.10, 12, and 24h) with the replacement of the same volume of fresh aerated receptor buffer. The solutions were filtered through a membrane filter (0.22μm) and were run on HPLC to quantify the content of EPR at each time interval.

The cumulative penetration Q was calculated by the following formula(5),

$$Q = \frac{V \times C_n + \sum_{i=1}^{n-1}(V_i \times C_i)}{A} \quad (5)$$

Where Cn represents the concentration of EPR in the receptor solution at the nth sampling point (μg/mL), V is the volume of the receptor pool (mL), Ci is the EPR concentration in the receptor solution at the ith (≤n-1) sampling point (μg/mL), Vi is the sampling volume (mL), and A is the effective diffusion area.

Linear regression was applied to the cumulative permeation Q against permeation time(t) to obtain the transdermal curve. The slope of this curve corresponds to the steady-state flux (J_{ss} $\mu g \cdot h^{-1} \cdot cm^{-2}$), and the intersection of the line with the X-axis represents the lag time (T_{lag}). The steady-state flux (J_{ss}) is a measure of the speed of drug transdermal absorption.

The apparent permeation coefficient (Papp) is calculated as Papp =J_{ss}/C_d, where Cd is the drug concentration in the administered dosage. This parameter evaluates the rate of drug transdermal absorption.

Dynamic Distribution Study of EPR in Skin

Confocal Raman spectroscopy was employed to determine the dynamic distribution of EPR in skin over time. At predetermined time intervals, the skin was removed.

Raman spectra of samples were collected by a confocal Raman Microscope (DXR. Thermo Fisher Scientific, Madison, USA) under a 50× objective, with the laser power at 8 mW. The exposure time was performed using 10 Hz and the laser spot size was estimated to be 3 μm. The number of scans was 100. To determine the distribution of EPR, the spectra were scanned downward from the adhesive layer of the patch to the skin with a 3μm step size for a total depth of 90μm. The spectra data was processed with OMNIC software. Difference skin samples were obtained by using the following manner(6),

$$\text{Difference spectra of skin} = \text{Spec}(2) - \text{Spec}(1) \quad (6)$$

Where Spec (1) was the spectrum of blank skin, Spec (2) was the spectrum of the skin sample. The peak at 1650 cm^{-1} was used to identify the intensity of EPR.

In vivo Experiments

Animals

Male Sprague-Dawley rats (250~300g) were sourced from the reputable Laboratory Animal Center of Jiangxi University of Traditional Chinese Medicine. Housed under controlled conditions, they maintained a 12-hour light-dark cycle and a temperature range of 20±2°C. Humidity was maintained at 50–60%, and they had constant access to standard chow and fresh water. Before oral administration, a 12-hour fast ensured optimal conditions for the procedure. All animal care and experimental protocols strictly adhered to established ethical guidelines and received prior approval from the China Pharmaceutical University Animal Ethical Experimentation Committee.

Pharmacokinetic Study of Eprinex and EPR Mixed Micelles

After collecting blood from the orbital sinus of rats, the whole blood was placed in sodium heparin tubes. The samples were then subjected to low-speed centrifugation (3500 rpm, 15 minutes) to obtain rat blank plasma. A volume of 100 μL of rat plasma was mixed with 400 μL of acetonitrile, vortexed for 5 minutes to precipitate proteins, and centrifuged at 4°C (10000 rpm, 15 minutes). The supernatant was collected for injection and peak area recording during analysis.

Ten SD (Latin name: Sprague Dawley) rats were randomly divided into two groups, the EPR micelle group (R1) and the Eprinex group (R2). Twenty-four hours before drug administration, the hair on both sides of the rat spine was shaved using a shaver, with a hair removal area of 6 cm × 6 cm. Subsequently, depilatory cream was applied and left for 30 seconds, followed by removal with warm water. The rats were fasted for 12 hours before dosing, during which they had access to water freely.

At a dose of 10 mg/kg, Eprinex and EPR Mixed micelles were evenly applied to the exposed skin of the shaved area. After administration, the dosing site was covered with a polyethylene wrap to prevent rats from licking, and the rats were

individually housed to avoid mutual interference that could result in the removal of the applied drugs. Blood samples were collected from the orbital sinus at 2, 4, 8, 10, 24, 26, 28, 32, 48, 72 and 96 hours post-dosing. The obtained whole blood was placed in heparinized tubes, and after centrifugation at 3500 rpm for 15 minutes, the plasma was separated and stored at −20°C for further use. A 100 μL aliquot of post-dosing plasma was processed according to the "Preparation of Plasma Samples" method. The processed plasma samples were then injected for analysis, and the peak area was recorded to calculate the blood drug concentration. The main pharmacokinetic parameters of EPR mixed micelles and EPR Eprinex were calculated using the non-compartmental model (NCA) in Phoenix® WinNonlin® 8.1, a software for pharmacokinetic/pharmacodynamic (PK/PD) and toxicokinetic industry modeling and simulation. The drug-time concentration curves for both formulations were also plotted.

Skin Irritation Test

A skin irritation test was conducted to determine the irritation safety level of the EPR micelle. In some cases, parasites would cause skin lesions, so it is necessary to investigate if there is any irritation of preparation to the damaged skin other than to the intact skin. For this, intact skin and damaged skin models were prepared according to the previous study. Briefly, 12 healthy male standard deviation SD rats (weight 200 ~220 g) were shaved on the back and were kept under observation for 24 h to check if any damage on the skin appeared. In case, any damage was found on the skin of any rat, was not involved in the study. After 24 h of observation, the shaved area on the back of rats was divided into two regions, one for intact and the other for damage. To develop the damaged region, a scalpel was used to make abrasion on the skin with a slight bloody appearance. After that, the rats were divided into five groups randomly, for control saline, blank micelle, EPR micelle, and Eprinex. The preparations were applied on both regions at 2 cm×2 cm area. All the animals were provided with the same ad libitum access at 25°C and 55% humidity room condition.

After completion of the 72 h study, the rats were sacrificed by cervical dislocation, and the skin samples from the test area were collected from the center part with an area of about 1 cm× 1 cm. The collected samples were preserved in 4% polyformaldehyde at 4 °C. The skins were embedded in paraffin and then sectioned into 5 μm thick sections and stained with H&E dye. The histological changes were imaged with a light microscope (Nikon, Tokyo, Japan).

Statistical Analysis

SPSS version 22.0 (SPSS Inc). was used for statistical analysis. *T*-test was used to analyze the significant difference (*P≤0.05, **P≤0.01). All data were expressed in mean±SD.

Results & Discussion

Determination of Critical Micelle Concentration (CMC)

The CMC, serving as a metric for the surface activity of surfactants, represents a pivotal point where notable changes occur in the solution properties. The physicochemical characteristics of surfactants undergo significant alterations before and after the formation of mixed micelles. Therefore, these changes can be harnessed to characterize the CMC of surfactants. Various methodologies are employed to determine the CMC and aggregation numbers of surfactants, including the surface tension method, conductivity method, light scattering method, and steady-state fluorescence probe method. In this study, the steady-state fluorescence method was employed to determine the CMC values of RH-40, NP-40, and the composite surfactant.

According to Figure 1, it can be seen that the CMC of RH-40 is 50.00 μg/mL, the critical micelle concentration of NP-40 is 568.539 μg/mL, and the critical micelle concentration of the mixed surfactant is 11.596 μg/mL.

Preparation and Characterization of Blank Mixed Micelles and EPR Mixed Micelles

The physicochemical properties of both Blank Mixed micelles and EPR Mixed micelles were evaluated. Dynamic light scattering (DLS) coupled with polydispersity index (PDI) determination revealed an average particle size of 13.87 nm ±0.10 and a PDI of 0.113 for Blank Mixed micelles (Figure 2A), indicating a moderately monodisperse population with minimal aggregation. The average particle size of 13.97±0.16 nm and a PDI of 0.132 for EPR Mixed micelles

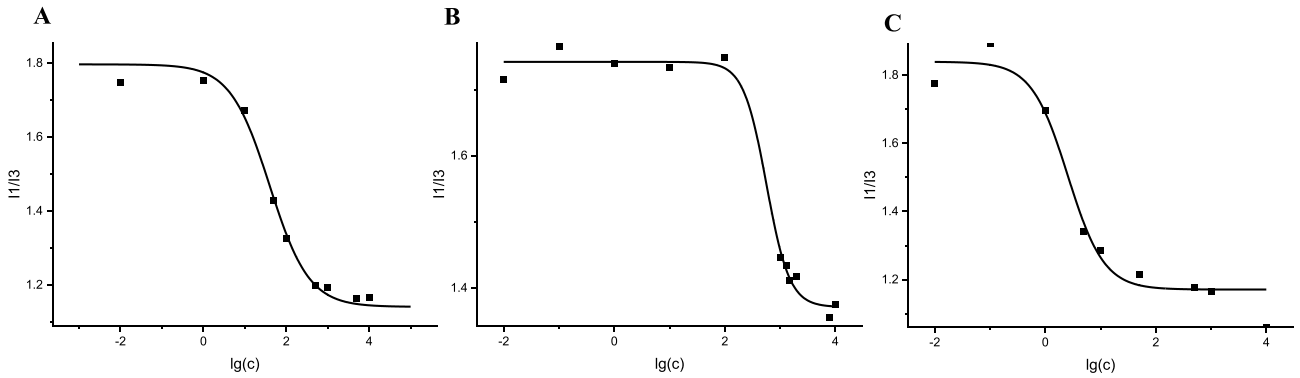

Figure 1 The CMC of RH-40 (**A**), NP-40 (**B**), Mixed RH-40 and NP-40 (**C**).

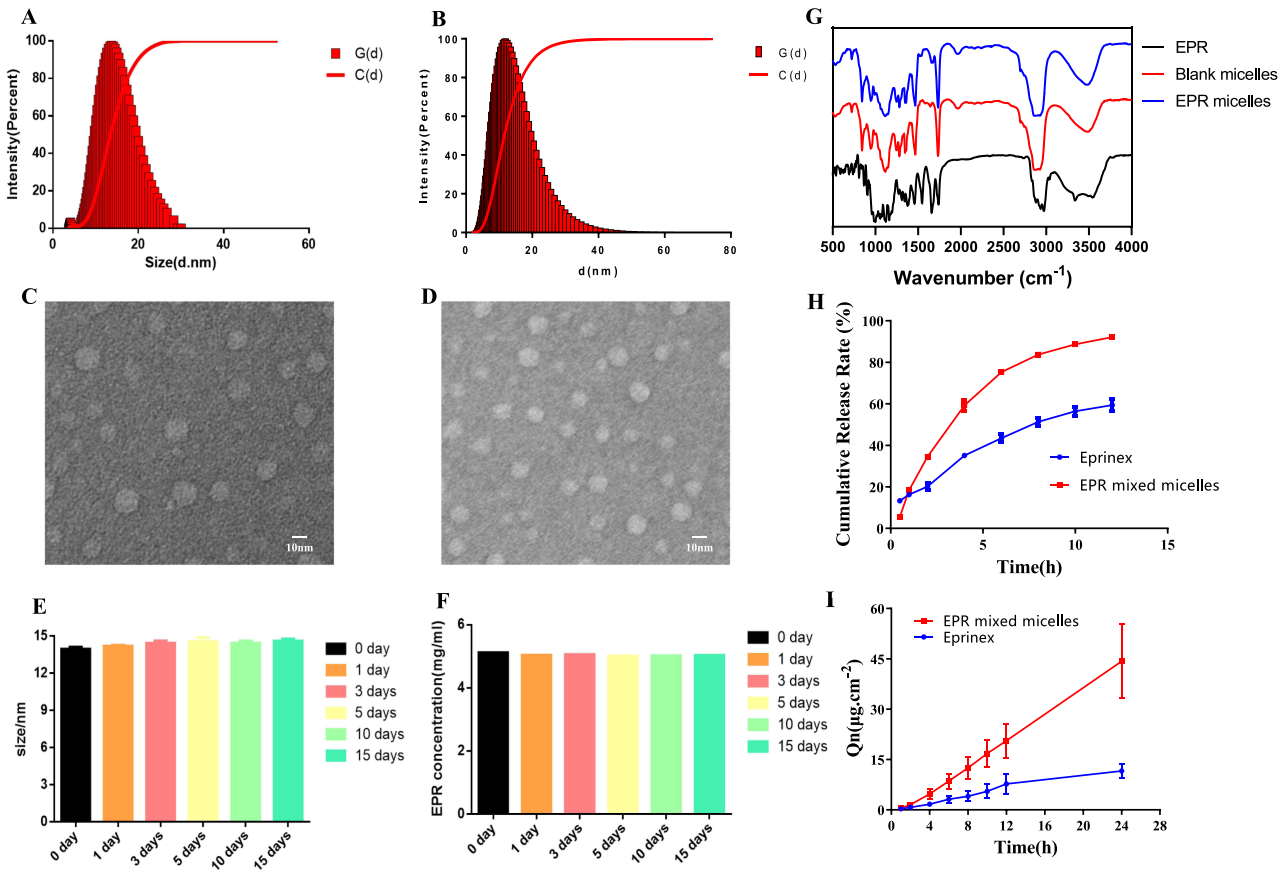

Figure 2 Preparation and Characterization of Blank mixed micelles and EPR mixed micelles. The size of Blank mixed micelles (**A**). The size of EPR mixed micelles (**B**). TEM images of Blank mixed micelles (**C**) and EPR mixed micelles (**D**). The size of EPR mixed micelles in 15 days (**E**). The EPR concentration of EPR mixed micelles in 15 days (**F**). The infrared spectroscopy of EPR raw material, Blank mixed micelles, and EPR mixed micelles (**G**). Drug release curves of Eprinex and EPR mixed micelles (**H**). Transdermal penetration curves of Eprinex and EPR mixed micelles (**I**).

(Figure 2B), indicating a moderately monodisperse population with minimal aggregation. Transmission electron microscopy (TEM) analysis (Figure 2C and D) corroborated this, showcasing the spherical morphology and uniform dispersion of Blank Mixed micelles and EPR Mixed micelles. Additionally, the spherical shape and thin layer of EPR coating the mixed micelles in the TEM image suggest good dispersion and successful conjugation. The drug loading efficiency of EPR was determined to be 0.49%. The encapsulation efficiency of EPR was determined to be 95.81%. The EPR mixed micelles exhibit good stability, with minimal changes in particle size and EPR content over 15 days (Figure 2E and F).

Ft-Ir

EPR mixed micelles contain EPR along with surfactants RH-40 and NP-40. Among these, EPR belongs to the class of macrolide compounds, characterized by functional groups such as carbonyl, acetylamino, and ester groups. Specific functional groups present in EPR include hydroxyl, carbonyl, aromatic structures, and oxide groups. In this experiment, infrared spectroscopy was employed to confirm the encapsulation of EPR within the mixed micelles. Therefore, infrared spectra were obtained for EPR raw material, blank mixed micelles, and EPR mixed micelles. The infrared spectra of these three substances are depicted in the Figure 2G. In the infrared spectrum of EPR raw material, characteristic absorption peaks of EPR were observed at three positions, namely 1656.82 cm^{-1}, 1004.89 cm^{-1}, and 3344.50 cm^{-1}, corresponding to the stretching vibrations of carbonyl, ester, and amino nitrogen-hydrogen bonds, respectively. A weak absorption peak of carbonyl vibration was observed at 1635.60 cm^{-1} in the infrared spectrum of blank mixed micelles. Additionally, the stretching vibration peak of the carbonyl group in the acetylamino group was also observed in the infrared spectrum of EPR mixed micelles at 1666.46 cm^{-1}, confirming the successful encapsulation of EPR within the mixed micelles.

In vitro Drug Release

EPR, as a poorly soluble drug, exhibits minimal solubility in physiological saline. According to the guiding principles of new drug research, for drugs with poor water solubility, it is common to incorporate certain amounts of organic solvents such as ethanol or isopropanol into the receptor buffer or add surfactants to enhance solubility. Regarding the receptor buffer, it is essential to ensure its sufficient capacity to dissolve the drug, meeting the sink conditions. Simultaneously, it is imperative to maintain the stability of the drug during long-term release to prevent degradation of its therapeutic efficacy.[30,31] As the in vitro drug release profiles indicate (Figure 2H), a more suitable vehicle for EPR release appears to be micelle, from which a 1.92-fold higher amount of the drug was released, comparing the Eprinex after 12 h. The liberation profiles show that the difference in the drug release occurs after approximately two hours when the drug amount released through the membrane begins to increase significantly compared to Eprinex. This is because the matrix used for dissolving the drug in Eprinex is oil-based, while EPR is a hydrophobic drug, making it difficult for the drug to be released from the matrix. The results showed that EPR permeated through the membrane at a constant rate and the diffusion behaviors were in accordance with Higuchi kinetics. The cumulative permeated amount of EPR from different formulations is listed in Table 1.

In vitro Permeation of Eprinex and EPR Mixed Micelles

In vitro experiments on transdermal penetration were carried out to investigate the effect of Eprinex and EPR mixed micelles on transdermal absorption of EPR. The results showed that EPR permeated through the skin at a constant rate and the diffusion behaviors were in accordance with zero-order kinetics. The cumulative permeated amount of EPR from different formulations is listed in Table 2. In the study, the Eprinex was designated as the control group, while the EPR mixed micelles were assigned as the experimental group. The time (Time, h) was plotted on the x-axis, and the cumulative permeation amount of EPR per unit area was plotted on the y-axis to generate a curve depicting the cumulative permeation amount per unit area for both formulations, as shown in Figure 2I. The cumulative permeation amount per unit area decreased in the following order, EPR mixed micelles > EPR Eprinex. The transdermal rate constant of EPR mixed micelles was 3.90 times that of the Eprinex.

Table 1 Drug Release Parameters of Different EPR Formulations (n=3, mean±SD)

Formulation	Equation	Jss ($\mu g \cdot cm^{-2} \cdot h^{-1}$)
Eprinex	Q_n= 411.2*√t-35.7, r^2 = 0.9891	411.2±28.75
EPR mixed micelles	Q_n= 740.7*√t-276.9, r^2= 0.9719	740.7±8.32**

Notes: **Indicates a significant difference between EPR mixed micelles and Eprinex (**p<0.01).

Table 2 Transdermal Penetration Parameters of Different EPR Formulations (n=4, mean±SD)

Formulation	Transdermal Curve Equation	J_{ss} (μg h^{-1} cm^{-2})	P_{app} ×10^5 (cm h^{-1})
EPR mixed micelles	Q_n = 1.933T - 2.5040	1.933±0.48**	3.86±0.95**
Eprinex	Q_n = 0.4959T - 0.3344	0.4959±0.093	0.99±0.19

Notes: **Indicates a significant difference between EPR mixed micelles and Eprinex (**p<0.01).

EPR Dynamic Distribution in Skin

Confocal Raman spectroscopy was employed to map the dynamic distribution of EPR in skin. Coherent anti-Stokes Raman spectroscopy (CARS) is an analytical technique used for transdermal penetration studies, based on the principle of Raman scattering. When a laser beam irradiates the sample surface, some photons interact with molecules, resulting in Raman scattering. The wavelengths of these scattered photons have slight shifts compared to the incident light, caused by molecular vibrations. CARS generates localized Raman spectra by focusing a laser beam on the sample surface, forming a tiny laser spot. Analyzing these spectral data allows for determining the distribution of drugs at different depths of the skin, as well as the extent of drug permeation and diffusion behavior in skin tissues, thereby elucidating the transdermal penetration mechanism of drugs. The 1650 cm^{-1} peak was identified to characterize EPR, based on which EPR relative intensities at different depths of skin were obtained over time as illustrated in Figure 3, the darker the color, the higher the drug concentration. When 0.5h after administration, the drug in the EPR micelle group quickly penetrated the skin, mainly distributed in 5 μm to 25 μm of the skin, while the drug permeability in the Eprinex group was less, when 1h after administration, the drug in the EPR micelle group and the Eprinex group penetrated the skin at 30μm to 55μm, but the drug concentration in the EPR micelle group was higher. When 6 hours after administration, the EPR micelles group drug penetrated the diffusion cell, and the drug was less retained in the skin, while the Eprinex drug was still retained in the skin. Most topical formulations, such as gels, ointments, creams, lotions, and patches, release drug molecules that need to pass through multiple layers of skin structures to enter the systemic circulation. Initially, drug molecules must diffuse through the lipophilic stratum corneum (SC), then penetrate through the aqueous-rich epidermis, and finally reach the capillaries in the dermis. Therefore, formulations for transdermal drug delivery need to possess both hydrophilic and lipophilic properties. If the molecules are too hydrophilic, they cannot penetrate the lipophilic SC; if they are too lipophilic, they cannot penetrate the water-rich epidermis.[32] Therefore, using amphiphilic EPR mixed micelles as carriers for transdermal drug delivery has certain advantages. This indicates that EPR mixed micelles have better permeability. The reasons for the good permeability of EPR mixed micelles may vary, (1) The non-ionic surfactants RH-40 and NP-40 in the mixed micelles enhance the fluidity of the stratum corneum lipids, disrupt the lipid bilayer structure, and enhance the permeability of the drug through the skin. (2) The particle size of EPR mixed micelles is less than 20 nm, allowing the drug to be transported to the absorption site through transcellular pathways, and nanoscale mixed micelles facilitate a larger surface contact area to maximize drug absorption through the skin. (3) Although the Eprinex contains nitrogen-containing penetration enhancers, the matrix of the Eprinex is oil-based, while EPR is a hydrophobic drug. Consequently, the drug is difficult to release from the matrix, thereby affecting its absorption.

Pharmacokinetic Study of Eprinex and EPR Mixed Micelles

The average drug-time curves of EPR mixed micelles and Eprinex after administration are shown in the Figure 4, it can be observed that the area under the average drug-time curve for EPR mixed micelles is greater than that for Eprinex. The key pharmacokinetic parameters of EPR mixed micelles and Eprinex are presented in the Table 3. The Tmax values for EPR mixed micelles and Eprinex are 25.33±1.15h and 26.00±3.46h, respectively, and the corresponding Cmax values are 5.80±2.08μg/mL and 2.99±0.89μg/mL. Although EPR mixed micelles have a smaller Tmax compared to Eprinex, the Cmax of EPR mixed micelles is greater. This indicates that the transdermal absorption of EPR mixed micelles is superior to that of Eprinex. The enhanced transdermal absorption of EPR mixed micelles, attributed to their smaller particle size,

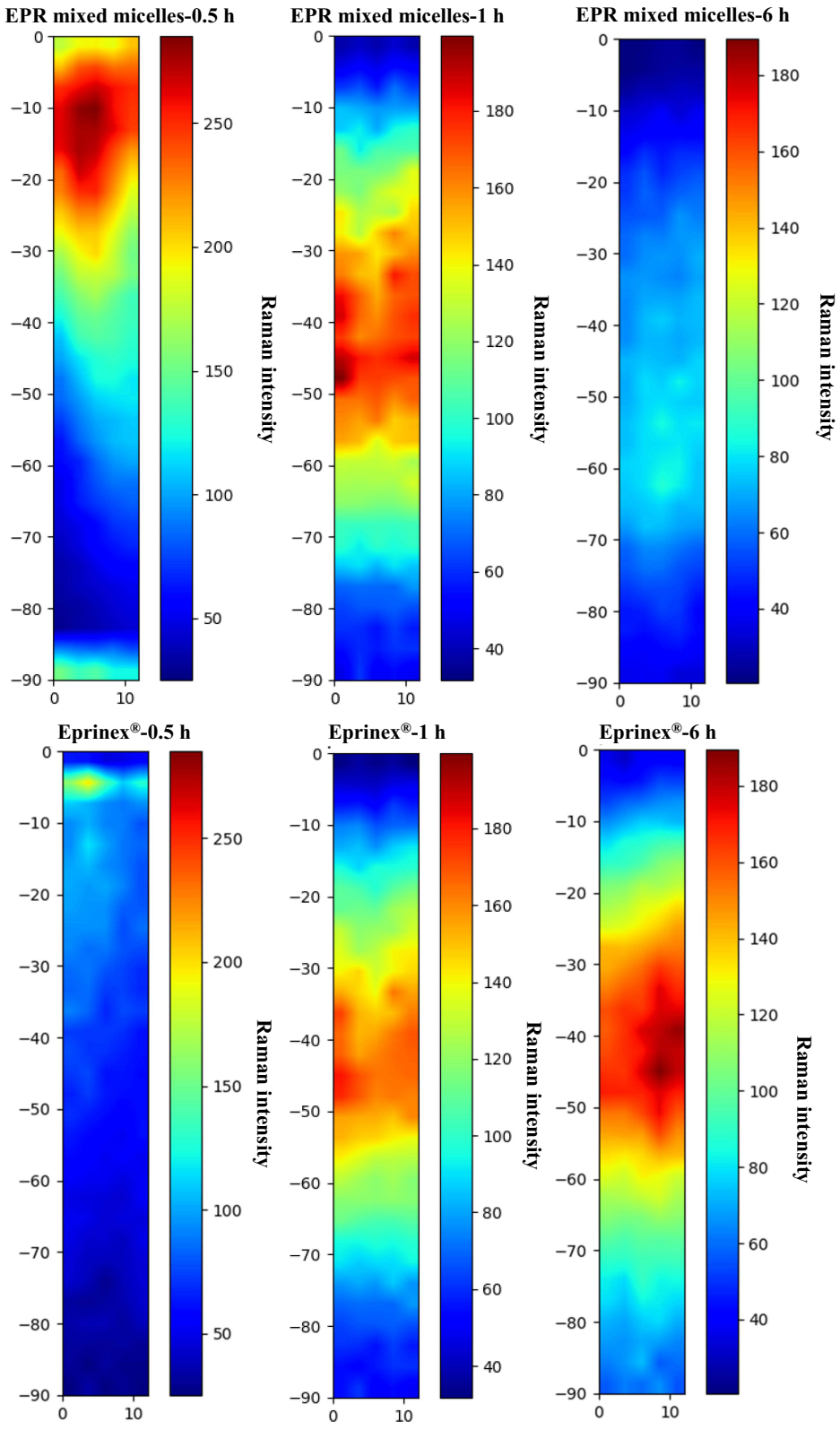

Figure 3 Transdermal penetration curves of Eprinex and EPR-Micelle.

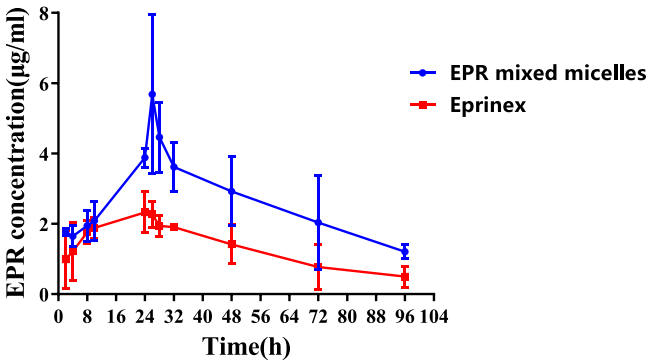

Figure 4 The concentration curve of EPR (n=3).

allows rapid penetration through the skin barrier and facilitates rapid drug release.[18,33] Additionally, the half-life and mean residence time of EPR mixed micelles are both greater than those of Eprinex, suggesting that the encapsulation of EPR in mixed micelles extends the duration of drug action. The AUC_{0-t} of EPR mixed micelles is approximately 2.11 times greater than that of Eprinex, while the $AUC_{0-\infty}$ of EPR mixed micelles is approximately 2.29 times greater than that of Eprinex. These results indicate an improvement in the transdermal absorption and bioavailability of EPR after encapsulation in mixed micelles formulations.

Skin Irritation Test

The safety of the EPR mixed micelles was further evaluated to ensure that it has low skin toxicity and cause negligible irritation to the skin. Histopathological knots (Figure 5A) showed that normal skin infiltrated with normal saline had no inflammation, epithelial cells were neatly aligned, collagen fibers in the dermis were regularly arranged, and no damage was observed in appendages such as hair follicle sebaceous glands. The damaged skin group had mild edema in the upper dermis with a single lymphocytic infiltrate (Figure 5B).

No significant inflammatory response was observed in the skin with different EPR prescriptions, indicating that the EPR prescription was not irritating to the skin of rats (Figure 5C). The skin of the control group had a small amount of inflammatory cell infiltration, while the damaged skin of EPR mixed micelles was intact after administration without obvious inflammatory reaction. Avermectin and its derivative ivermectin have been reported to have anti-inflammatory effects. Because EPR is a derivative of avermectin, it may also have anti-inflammatory effects. The tissue sections of Eprinex showed inflammation and possessed a certain degree of irritation, likely due to the presence of a large amount of penetration enhancers, which can cause damage to the skin. The overall results suggest that EPR mixed micelles are within the skin tolerance range and are safe for transdermal administration.

Table 3 Pharmacokinetic Parameters of EPR-Micelle and Eprinex in Rats (mean±SD, n=3)

Parameters	Unit	EPR-Micelle	Eprinex
Tmax	h	25.33±1.15	26.00±3.46
Cmax	μg/mL	5.80±2.08*	2.99±0.89
T1/2	h	34.70±10.23	28.016±8.49
AUC_{0-t}	h·μg/mL	244.62±53.19*	116.03±18.48
$AUC_{0-\infty}$	h·μg/mL	306.83±79.98*	133.66±20.16
MRT	h	42.313±5.41	36.49±2.42

Notes: *Indicates a significant difference between EPR mixed micelles and Eprinex (*p<0.05).

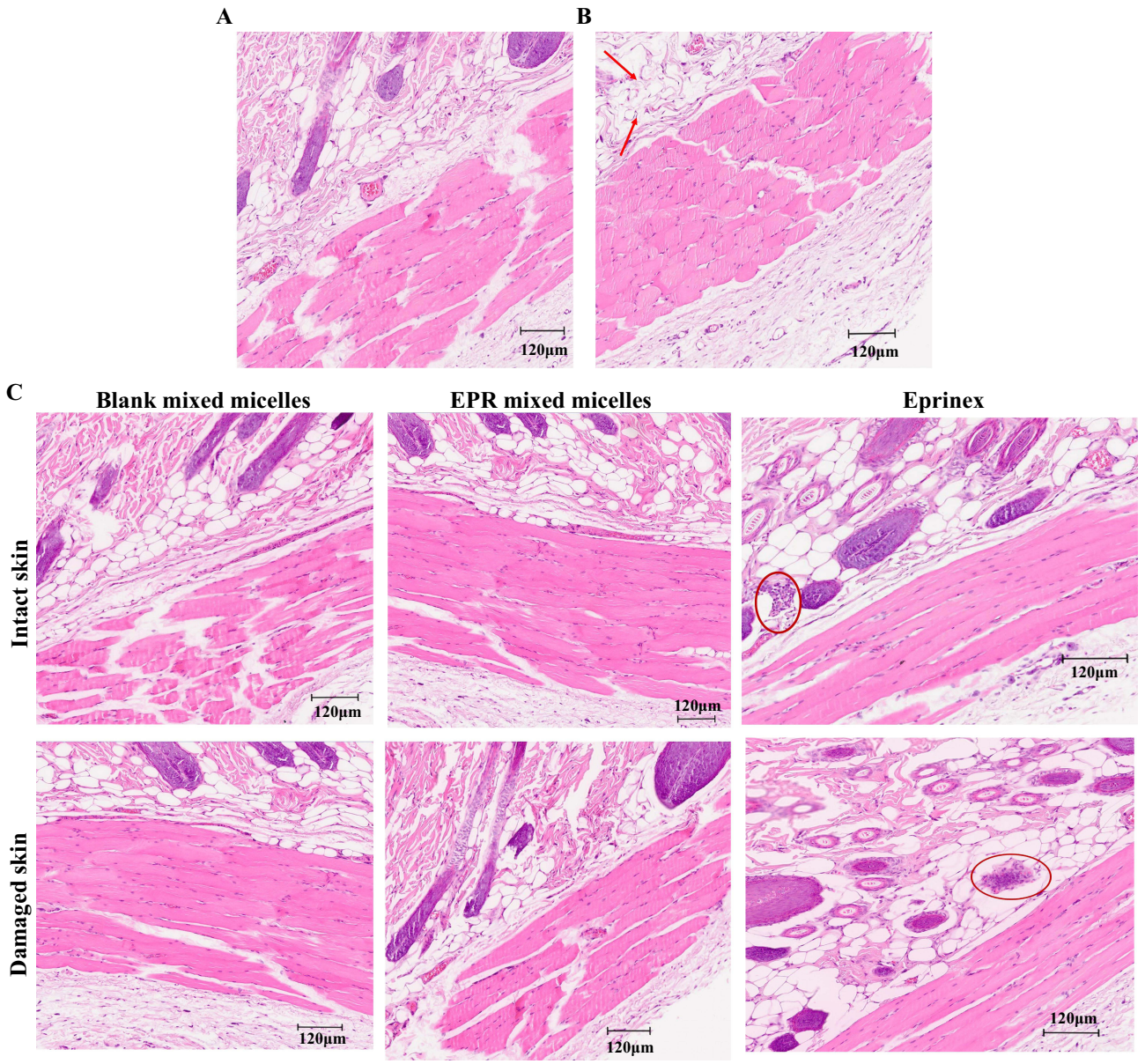

Figure 5 Skin irritation test results. H&E staining of intact skin (**A**) and damaged skin (**B**) applied with normal saline, intact skin, and damaged skin applied with different formulations (**C**) for 72h. Arrows indicate the edema and ellipse indicates infiltration of inflammatory cells.

Conclusion

This study aims to develop a novel EPR mixed micelle by optimizing the preparation process and characterization methods. The research investigates its transdermal performance in vitro, safety in vivo, and pharmacokinetic characteristics, with the goal of providing new solutions for the prevention and control of parasitic diseases as well as animal health management.

Through preliminary formulation studies and optimization of the preparation process, this research successfully produced stable EPR mixed micelles with suitable particle sizes. Multiple characterization techniques were employed to validate their physicochemical properties. In terms of transdermal performance evaluation, the EPR mixed micelles exhibited favorable drug release characteristics, demonstrating higher transdermal rates and permeation amounts compared to the commercially available pour-on agent Eprinex. This provides strong evidence for their clinical application; however, it is important to note that this study did not investigate the specific pathways through which these mixed micelles penetrate into the skin. Further research is needed to explore these penetration mechanisms.

Additionally, safety assessments and pharmacokinetic studies conducted using animal models confirmed that EPR mixed micelles possess good safety profiles in rats. Furthermore, they demonstrated higher absorption rates and drug concentrations than those observed with the pour-on agent Eprinex, offering valuable reference data for their application in animals. Nonetheless, both safety evaluations and comprehensive efficacy against parasites require further refinement within this context to provide robust support for clinical applications of EPR mixed micelles.

Acknowledgments

This work was supported by Jiangsu Agri-Animal Husbandry Vocational College (Grant No.NSF2022ZR04).

Disclosure

The authors report no conflicts of interest in this work.

References

1. Cable J, Barber I, Boag B, et al. Global change, parasite transmission and disease control: lessons from ecology. *Philos Trans R Soc London, Ser B*. 2017;372:1719.
2. Sun Y, Chen D, Pan Y, et al. Nanoparticles for antiparasitic drug delivery. *Drug Delivery*. 2019;26(1):1206–1221. doi:10.1080/10717544.2019.1692968
3. Packianathan R, Hodge A, Wright J, Pearce M, DeRosa AA. Efficacy of a fixed-dose combination injectable (0.2 mg/kg doramectin + 6.0 mg/kg levamisole hydrochloride) in Australian cattle against naturally acquired gastrointestinal nematode infections. *Vet Parasitol*. 2023;323:110025. doi:10.1016/j.vetpar.2023.110025
4. Momčilović S, Cantacessi C, Arsić-Arsenijević V, Otranto D, Tasić-Otašević S. Rapid diagnosis of parasitic diseases: current scenario and future needs. *Clin Microbiol Infectio*. 2019;25(3):290–309. doi:10.1016/j.cmi.2018.04.028
5. Ricciardi A, Ndao M. Diagnosis of parasitic infections: what's going on? *J Biomol Screen*. 2015;20(1):6–21. doi:10.1177/1087057114548065
6. Hamame A, Davoust B, Cherak Z, Rolain JM, Diene SM. Mobile Colistin Resistance (mcr) Genes in Cats and Dogs and Their Zoonotic Transmission Risks. *Pathogens*. 2022;11:6. doi:10.3390/pathogens11060698
7. Shoop WL, DeMontigny P, Fink DW, et al. Efficacy in sheep and pharmacokinetics in cattle that led to the selection of eprinomectin as a topical endectocide for cattle. *Internat J Parasitol*. 1996;26(11):1227–1235. doi:10.1016/S0020-7519(96)00122-1
8. Gogolewski RP, Slacek B, Familton AS, et al. Efficacy of a topical formulation of eprinomectin against endoparasites of cattle in New Zealand. *New Zealand Veterin J*. 1997;45(1):1–3. doi:10.1080/00480169.1997.35978
9. Shoop W, Michael B, Egerton J, Mrozik H, Fisher M. Titration of subcutaneously administered eprinomectin against mature and immature nematodes in cattle. *J Parasitol*. 2001;87(6):1466–1469. doi:10.1645/0022-3395(2001)087[1466:TOSAEA]2.0.CO;2
10. Hinney B, Wiedermann S, Kaiser W, Krücken J, Joachim A. Eprinomectin and Moxidectin Resistance of Trichostrongyloids on a Goat Farm in Austria. *Pathogens*. 2022;11:5. doi:10.3390/pathogens11050498
11. Cringoli G, Rinaldi L, Veneziano V, Capelli G. Efficacy of eprinomectin pour-on against gastrointestinal nematode infections in sheep. *Vet Parasitol*. 2003;112(3):203–209. doi:10.1016/S0304-4017(03)00007-4
12. Shoop WL, Egerton JR, Eary CH, et al. Eprinomectin: a novel avermectin for use as a topical endectocide for cattle. *Internat J Parasitol*. 1996;26(11):1237–1242. doi:10.1016/S0020-7519(96)00123-3
13. Merola VM, Eubig PA. Toxicology of avermectins and milbemycins (macrocylic lactones) and the role of P-glycoprotein in dogs and cats. *Veter Clin North Am Small Animal Pract*. 2012;42(2):313–33,vii. doi:10.1016/j.cvsm.2011.12.005
14. Rehbein S, Hamel D, Yoon S, Johnson C. Efficacy of eprinomectin topical solution and eprinomectin extended-release injection treatments against developing larval and adult Chabertia ovina and Oesophagostomum venulosum - two less common cattle nematode parasites. *Vet Parasitol*. 2022;312:109837. doi:10.1016/j.vetpar.2022.109837
15. Ranade VV. Drug delivery systems. 6. Transdermal drug delivery. *J Clin Pharmacol*. 1991;31(5):401–418. doi:10.1002/j.1552-4604.1991.tb01895.x
16. Chatterjee B, Reddy A, Santra M, Khamanga S. Amorphization of Drugs for Transdermal Delivery-a Recent Update. *Pharmaceutics*. 2022;14:5. doi:10.3390/pharmaceutics14050983
17. Neupane R, Boddu SHS, Abou-Dahech MS, et al. Transdermal delivery of chemotherapeutics: strategies, requirements, and opportunities. *Pharmaceutics*. 2021;13:7. doi:10.3390/pharmaceutics13070960
18. Mao Y, Chen X, Xu B, et al. Eprinomectin nanoemulgel for transdermal delivery against endoparasites and ectoparasites: preparation, in vitro and in vivo evaluation. *Drug Delivery*. 2019;26(1):1104–1114. doi:10.1080/10717544.2019.1682720
19. Zhang D, Zhang K, Gao J, et al. Anthelmintic efficacy, plasma and milk kinetics of eprinomectin following topical and subcutaneous administration to yaks (Bos grumniens). *Exp Parasitol*. 2015;153:17–21. doi:10.1016/j.exppara.2015.02.010
20. Hoste H, Lespine A, Lemercier P, Alvinerie M, Jacquiet P, Dorchies P. Efficacy of eprinomectin pour-on against gastrointestinal nematodes and the nasal bot fly (Oestrus ovis) in sheep. *Veterin Record*. 2004;154(25):782–785. doi:10.1136/vr.154.25.782
21. Hamel D, Visser M, Mayr S, et al. Eprinomectin pour-on: prevention of gastrointestinal and pulmonary nematode infections in sheep. *Vet Parasitol*. 2018;264:42–46. doi:10.1016/j.vetpar.2018.11.002
22. Termatzidou SA, Arsenopoulos K, Siachos N, et al. Anthelmintic activity of injectable eprinomectin (eprecis(®) 20 mg/mL) in naturally infected dairy sheep. *Vet Parasitol*. 2019;266:7–11. doi:10.1016/j.vetpar.2018.12.014
23. Makhmalzade BS, Chavoshy F. Polymeric micelles as cutaneous drug delivery system in normal skin and dermatological disorders. *J Adv Pharmaceut Technol Res*. 2018;9(1):2–8. doi:10.4103/japtr.JAPTR_314_17
24. Lapteva M, Santer V, Mondon K, et al. Targeted cutaneous delivery of ciclosporin A using micellar nanocarriers and the possible role of inter-cluster regions as molecular transport pathways. *J Control Rel*. 2014;196:9–18. doi:10.1016/j.jconrel.2014.09.021

25. Lapteva M, Mondon K, Möller M, Gurny R, Kalia Y. Polymeric micelle nanocarriers for the cutaneous delivery of tacrolimus: a targeted approach for the treatment of psoriasis. *Mol Pharmaceut*. 2014;11:2989–3001. doi:10.1021/mp400639e
26. Bachhav YG, Mondon K, Kalia YN, Gurny R, Möller M. Novel micelle formulations to increase cutaneous bioavailability of azole antifungals. *J Control Release*. 2011;153(2):126–132. doi:10.1016/j.jconrel.2011.03.003
27. Lapteva M, Möller M, Gurny R, Kalia YN. Self-assembled polymeric nanocarriers for the targeted delivery of retinoic acid to the hair follicle. *Nanoscale*. 2015;7(44):18651–18662. doi:10.1039/C5NR04770F
28. Dahmana N, Mugnier T, Gabriel D, et al. Polymeric micelle mediated follicular delivery of spironolactone: targeting the mineralocorticoid receptor to prevent glucocorticoid-induced activation and delayed cutaneous wound healing. *Int J Pharm*. 2021;604:120773. doi:10.1016/j.ijpharm.2021.120773
29. Hornof M, Toropainen E, Urtti A. Cell culture models of the ocular barriers. *Europ J Pharmaceut Biopharmac*. 2005;60(2):207–225. doi:10.1016/j.ejpb.2005.01.009
30. Medlicott NJ, Waldron NA, Foster TP. Sustained release veterinary parenteral products. *Adv. Drug Delivery Rev.* 2004;56(10):1345–1365. doi:10.1016/j.addr.2004.02.005
31. Piotrowicz A, Shoichet MS. Nerve guidance channels as drug delivery vehicles. *Biomaterials*. 2006;27(9):2018–2027. doi:10.1016/j.biomaterials.2005.09.042
32. Yu YQ, Yang X, Wu XF, Fan YB. Enhancing permeation of drug molecules across the skin via delivery in nanocarriers: novel strategies for effective transdermal applications. *Front Bioeng Biotechnol*. 2021;9:646554. doi:10.3389/fbioe.2021.646554
33. Zhou Y, Wang C, Liu W, Yang M, Xu B, Chen Y. Fast in vitro release and in vivo absorption of an anti-schizophrenic drug paliperidone from its Soluplus(®)/TPGS mixed micelles. *Pharmaceutics*. 2022;14:5. doi:10.3390/pharmaceutics14050889